Why Oxonium Cation in the Crystal Phase is a Bad Acceptor of Hydrogen Bonds: A Charge Density Analysis of Potassium Oxonium Bis(hydrogensulfate)

Yulia V. Nelyubina,[†] Sergey I. Troyanov,[‡] Mikhail Yu. Antipin,[†] and Konstantin A. Lyssenko*,[†]

A.N. Nesmeyanov Institute of Organoelement Compounds, Russian Academy of Sciences, 119991, Vavilov Str., 29, Moscow, Russia, and Moscow State University, 119991, Vorob'evy Gory, 1, Moscow, Russia

Received: January 9, 2009; Revised Manuscript Received: March 4, 2009

Peculiarities of chemical bonding in the crystal of potassium oxonium bis(hydrogensulfate) were analyzed by means of R. Bader's "Atoms in Molecule" theory on the basis of the experimental data. The results obtained were shown to provide insight into the tendency of the oxygen atom of the oxonium moiety to avoid the H-bond formation in its crystalline salts.

Introduction

Hydrogen bonds are the strongest of all the noncovalent interactions.[1−3] This type of bonds is the main tool for controlling supramolecular assembly in solids.[4−6] In this context, the oxonium cation, playing the key role in proton transfer[7] processes, can be regarded one of the most important ionic species. It is a very convenient proton donor owing to the acidic nature of its hydrogen atoms. However, the acceptor abilities of H_3O^+ are very poor; the search in the Cambridge Structural Database (CSD)[8] has reveled that the oxonium cation mainly participates in weak $C-H\cdots OH_3^+$ bonding. Only in some cases the nondirectional $O-H\cdots OH_3^+$ contacts were formed in crystals exposed to high pressure.[9] Such behavior of the oxonium ion can be partly explained through the electrostatic considerations of the H-bonding. The withdrawal of a charge density from the oxygen atom by an additional proton makes it a less effective acceptor site compared to water molecule. On the other hand, in the bound state the atomic charges for the oxonium moiety are clearly affected by the charge transfer from its counterion.[2] The absence of the H-bonds involving the oxygen atom of H_3O^+ can be also the result of the compact character of its lone pair. This agrees with the relatively high HOH angle values in the oxonium ion, which are 111−113° for the half of oxonium-containing structures (ordered, with $R < 0.075$) found in CSD.[8] For comparison, the analogous value for the NH_3 moiety[10] is clearly smaller and falls into the range of 105−110°.

To check the above assumptions on the H-bonding behavior of the oxonium cation, we have carried out a high-resolution X-ray diffraction study of the electron density distribution function $\rho(\mathbf{r})$[11−13] in the crystalline potassium oxonium bis(hydrogensulfate) (**1**).[14] Analysis of these data within R. Bader's "Atoms in Molecules" (AIM) topological theory[15] allows one to localize the interatomic interactions and lone pair domains in solids based on the presence of the critical points (CP), CP (3, −1) in $\rho(\mathbf{r})$ and CP (3, −3) in $\nabla^2\rho(\mathbf{r})$ functions,[15] respectively. At the same time, it makes possible evaluating the charges and other quantitative characteristics[16,17] of atoms. Accordingly, using the AIM approach we were also able to estimate the influence of H-bond formation, involving H atoms of the oxonium, on the charge redistribution over the entire oxonium moiety in the solid. The possibility to calculate the energy of interactions on the basis of the experimental data enables a detailed comparison of the K−O and $O_{ox}-H\cdots O$ bonds as well as that of two symmetrically nonequivalent SO_4H^- species in the crystal of **1** (part A of Figure 1).

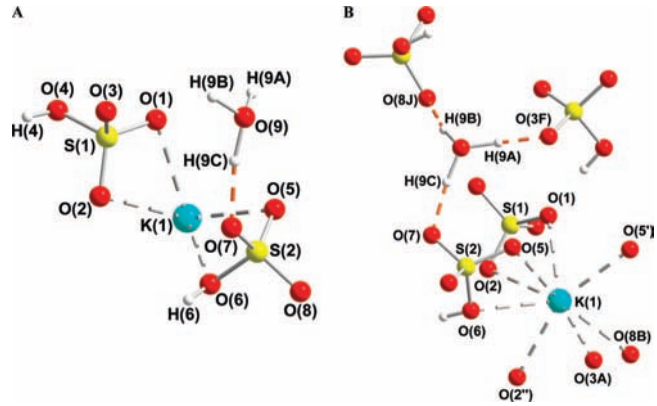

Figure 1. Independent part of unit cell in **1** (**A**), first coordination sphere of the potassium atom and the H-bonds with the oxonium cation (**B**).

Experimental Section

Crystals of **1** ($H_5KO_9S_2$, M = 252.26) are monoclinic, space group $P2_1/c$, at 120 K: a = 7.144(3), b = 13.560(7), c = 8.418(4) Å, β = 105.19(4)°, V = 787.0(7) Å^3, Z = 2 (Z' = 1), d_{calcd} = 2.129 gcm^{-3}, μ(Mo Kα) = 12.25 cm^{-1}, F(000) = 512. Intensities of 18 304 reflections were measured with a Syntex $P2_1$ diffractometer [λ(Mo Kα) = 0.71072Å, $\theta/2\theta$ -scans, $2\theta <$ 100°] and 8070 independent reflections [R_{int} = 0.0274] were used in further refinement. The structure was solved by direct method and refined by the full-matrix least-squares technique against F^2 in the anisotropic−isotropic approximation. Hydrogen atoms were located from the Fourier synthesis of the electron density and refined in the isotropic approximation. For **1**, the refinement converged to wR2 = 0.0687 and GOF = 1.000 for all independent reflections (R1 = 0.0276 was calculated against F for 5572 observed reflections with $I > 2\sigma(I)$). All calculations were performed using *SHELXTL PLUS 5.0*.[18] CSD 420244 contains the supplementary crystallographic data for **1**. These data can be obtained free of charge from Fachinformationszentrum Karlsruhe, 76344 Eggenstein-Leopoldshafen, Germany

* To whom correspondence should be addressed. E-mail: kostya@xrlab.ineos.ac.ru.
† Russian Academy of Sciences.
‡ Moscow State University.

10.1021/jp900215h CCC: $40.75
Published on Web 04/01/2009

TABLE 1: Atomic Charges and Volumes for atoms in 1[a]

atom	q, e	Vat, Å^3	atom	q, e	Vat, Å^3
K(1)	+0.85	18.99	O(6)	−0.81	15.10
S(1)	+3.43	4.93	O(7)	−0.85	14.64
O(1)	−0.94	15.59	O(8)	−1.00	15.94
O(2)	−1.52	19.56	H(6)	+0.40	2.47
O(3)	−1.11	17.94	O(9)	−1.04	18.87
O(4)	−1.07	16.45	H(9A)	+0.44	2.43
H(4)	+0.55	2.51	H(9B)	+0.51	2.12
S(2)	+3.28	5.38	H(9C)	+0.38	3.03
O(5)	−1.48	21.64			

[a] The value of the charge leakage is only 0.02 e. The sum of atomic volumes (196.01 Å^3) reproduces well the unit cell volume per independent part (196.73 Å^3) with relative error 0.4%. Although the integrated Langrangian ($L(\mathrm{r}) = -1/4\nabla^2\rho(\mathbf{r})$) for every $\mathbf{\Omega}$ has to be exactly zero,[15] reasonably small numbers with averaged value of 0.08×10^{-4} au and maximum L(r) observed for S(2) atom (0.3×10^{-4} au) were obtained.

(fax: (+49)7247−808−666; e-mail: crysdata@fiz-karlsruhe.de, http://www.fiz-karlsruhe.de/ecid/Internet/en/DB/icsd/depot_anforderung.html).

The multipole refinement was carried out within the Hansen-Coppens formalism[19] using *XD* program package[20] with the core and valence electron density derived from wave functions fitted to a relativistic Dirac−Fock solution.[21] Before the refinement, the O−H bond distances for hydrogensulfate and oxonium ions were normalized to the values of 0.87 and 1.08 Å obtained from the statistical analysis of similar structures. The level of multipole expansion was octupole for potassium, sulfur, and oxygen atoms. The dipole D_{10} was refined for hydrogen atoms. The refinement was carried out against F and converged to $R = 0.0202$, Rw = 0.0230, and GOF = 0.88 for 4741 merged reflections with $I > 3\sigma(I)$. All bonded pairs of atoms satisfy the Hirshfeld rigid-bond criteria (difference of the mean square displacement amplitudes along the bonds was not larger than 11×10^{-4} Å^2). The potential energy density v(**r**) was evaluated through the Kirzhnits approximation[22] for the kinetic energy density function g(**r**). Accordingly, the g(**r**) function is described as $({}^3/_{10})(3\pi^2)^{2/3}[\rho(\mathbf{r})]^{5/3} + ({}^1/_{72})|\nabla\rho(\mathbf{r})|^2/\rho(\mathbf{r}) + {}^1/_6\nabla^2\rho(\mathbf{r})$, what in conjunction with the local virial theorem ($2\ g(\mathbf{r}) + v(\mathbf{r}) = {}^1/_4\nabla^2\rho(\mathbf{r})$) leads to the expression for v(**r**) and makes it possible to estimate the electron energy density $h_e(\mathbf{r})$. The total electron density function was positive everywhere. The maximum (not more than 0.22 eÅ^{-3}) and minimum (−0.30 eÅ^{-3}) of the residual electron density were located in the vicinity of the potassium K(1) and sulfur S(2) nuclei, respectively. Analysis of topology of the $\rho(\mathbf{r})$ function was carried out using the *WINXPRO* program package.[23]

Results and Discussion

Examination of the crystal packing (part B of Figure 1) revealed that the potassium cation in the solid **1** is surrounded by six SO_4H^- anions comprising three of each nonequivalent SO_4H^-. One of them forms two K−O bonds, whereas two others − only one. Thus, the coordination number for K atom is 8. The potassium to oxygen distances for all the K−O interactions fall into the range of 2.6906(11) − 2.9657(12) Å (Table 1). Its average value is practically the same for $S(1)O_4H^-$ and $S(2)O_4H^-$ anions (2.791 and 2.801 Å). Although in terms of the metal−anion binding the independent hydrogensulfate species are quite similar, the difference between them can be found when considering the second coordination sphere of the potassium atom. Thus, the smallest K−O distance to the oxygen atom of the next nearest $S(2)O_4H^-$ hydrogensulfate is 3.385(2) Å, whereas for $S(1)O_4H^-$ it increases up to 4.035(2) Å. This also concerns the H-bonded patterns of the two anions. The $S(1)O_4H^-$ species are assembled into infinite chains via O−H···O bonds (O(4)···O(1) 2.595(2) Å, OHO 175(1)°) and the $S(2)O_4H^-$ ones in the crystal form centrosymmetric dimers (O(6)···O(7) 2.648(2) Å, OHO 174(1)°). The independent hydrogensulfate anions do not directly interact with each other, which allows neglecting their mutual influence. The above supramolecular associates are held together by the H-bonds with the H_3O^+ cation; the interatomic O_{ox}···O separation is in the range of 2.530(2)−2.674(2) Å. Moreover, each oxonium acting as a proton donor binds to only one $S(1)O_4H^-$ moiety and to two symmetrically equivalent anions of the second type. There is no H-bond connecting a hydrogen atom with the oxygen of the oxonium in the crystal of **1**.

To check if the poor H-bonding ability of the oxonium cation depends mainly on the electrostatic component of the H-bonds, we estimated the atomic charges (q_{at}) by integration of $\rho(\mathbf{r})$ over $\mathbf{\Omega}$, the atomic basins surrounded by zero-flux surface.[15] The obtained values indicate that because of the charge transfer accompanying the H-bond formation[2] the net charge of the oxonium moiety is only +0.25 e. Although the third proton in H_3O^+ should withdraw the charge density from the oxygen atom, the occurrence of the additional O_{ox}−H···O bond with the anion compensates for it. The q_{at} value for the O(9) oxygen reaches −1.0 e (Table 1), which is not so far from that in water molecule. For instance, the same parameter in the crystalline piperidine-2-carboxylic acid tetrahydrate[24] is about −1.4 e but in this case the entire water molecules are to some extent negatively charged. Moreover, in the crystal of $[GdCl_1Phen_2(H_2O)_3]Cl_2(H_2O)$ complex[25] the oxygen charge for unbound water molecule was only −0.9 e with the overall value being −0.1 e. Hence, the smaller negative charge of the O_{ox} atom, even though it somewhat contributes to the absence of H-bonds involving the H_3O^+ moiety as a proton acceptor, does not play the decisive role in this phenomenon.

The further examination of atomic characteristics revealed that the net charges (q_{an}) as well as the volumes (V_{an}) of the two independent anions are different. The corresponding q_{an} and V_{an} values for the $S(1)O_4H^-$ moiety are −0.66 e and 76.98 Å^3, whereas for the $S(2)O_4H^-$ one they are equal to −0.46 e and 75.17 Å^3. Such difference is, apparently, due to the variation of a cation−anion H-bonds strength because the K−O interactions for the two hydrogensulfate species are geometrically similar and have little effect on the anions (the q_{at} for potassium exceeds +0.85 e).

To estimate the energy of the H-bonds and, thus, to explain the observed charge transfer in the crystal of **1**, we have performed a search for CPs (3, −1), bond critical points or BCPs, in the interionic area. As a result, the BCPs within the fist coordination sphere of the potassium atom were found only for 7 potassium−anion interactions expected on the basis of the geometrical criteria. The exception is the K(1)−O(5) bond (K···O 2.9475(14) Å), which links the metal cation and the oxygen atom belonging to the same independent part. It should be mentioned that this was also observed in the crystal of potassium hydrophthalate,[26] where the K−O separation of 2.9565(3) Å did not correspond to the bonding interaction. The absence of the BCP for the K(1)−O(5) contact in **1**, however, agrees with the distribution of the static deformation electron density (DED) in the relevant plane. Although the DED map (Figure 2) is characterized by the common features: the accumulation of the electron density in the covalent bonding regions and in the vicinity of oxygens (attributed to their lone

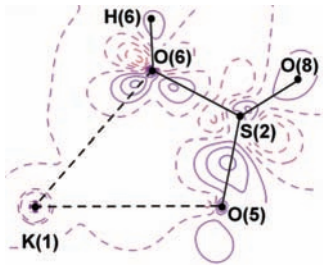

Figure 2. Section of the static deformation electron density (DED) function in the plane of the K(1), O(5), and O(6) atoms in **1**. Contours are drawn with 0.1 eÅ^{-3} step, the nonpositive contours are dashed.

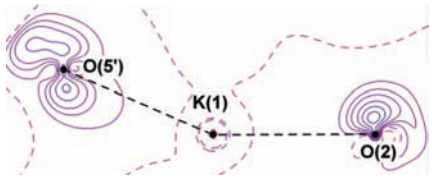

Figure 3. The DED distribution in the section of the K(1)−O(2) and K(1)−O(5′) bonds (the atom with asterisk is obtained from the basic one via the symmetry operation $-x+1, -y+1, -z+1$) in the crystal of **1**. The contours are drawn with 0.1 eÅ^{-3} step, the nonpositive contours are dashed.

pairs (LPs)), the LP domain of the O(5) atom significantly deviates from the K(1)O(5)O(6) plane and, in particular, from the K−O line. In the case of the true K−O bonds (Figure 3), the LPs of oxygen atoms are to a great extent directed toward the area of an electron density depletion around the potassium (peak-to-hole type) in a similar manner as it was observed for the Na−O interactions in the crystal of sodium iodide dihydrate.[27] This is indicative of the M−O bonds formation via the charge transfer from the oxygen's LPs to the metal atom. In contrast, the DED distribution for the K(1)−O(5) contact in **1** cannot be described in terms of the peak-to-hole formalism.

According to the topological parameters of $\rho(\mathbf{r})$ function in the BCPs of the metal−anion bonds ($\rho(\mathbf{r}) = 0.070 - 0.177$ eÅ^{-3}, the $\nabla^2\rho(\mathbf{r})$ values and the electron energy densities $h_e(\mathbf{r})$ are positive and equal to 0.71−1.94 eÅ^{-5} and 0.00035−0.00484 au, respectively) the latter belong to the closed-shell type of interatomic interactions.[15] This together with the small value of the charge transfer in **1** indicate the relative weakness of the K−O bonds. To characterize it on the quantitative level, we have estimated the K−O bond energy using the Espinosa's correlation scheme[16,17] − the semiquantitive relationship between the energy of an interaction (E_{int}) and the value of the potential energy density function v(**r**) in its BCP. The latter is not only valid for weak interactions such as H···H, C−H···O contacts but also for Mg···C, Ca···C,[28,29] moderate and strong H-bonds,[30,31] Au-PPh$_3$[32] and Gd−OH$_2$[25] bonds corresponding to intermediate type of interatomic interactions. The energy of the K−O bonds in **1** was found to be in the range of 2.5 − 5.9 kcal/mol (Table 2). For comparison, the same value in the above potassium hydrophthalate ranges from 0.35 kcal/mol (for the additional coordination bond, K···O 3.5120(3) Å) to 4.8 kcal/mol, and the energy of only one anion−anion H-bond exceeds that for all the K−O interactions.[26]

The topological analysis of $\rho(\mathbf{r})$ function in the interatomic area between the anions and the oxonium moiety in the crystalline **1** revealed the BCPs for the above H-bonds and for a number of additional O···O interactions (Table 2). The DED distributions for the former (Figures 4 and 5) are typical for the classical H-bonds,[33] that is the DED peaks attributed to the LPs of oxygen atoms are directed toward the hydrogens of proton-donor moieties. Although the type of these interactions varies from the intermediate to the closed-shell one ($\nabla^2\rho(\mathbf{r})$ and $h_e(\mathbf{r})$ in the BCPs are 2.34−5.71 eÅ^{-5} and −0.01669−0.09344 au), the high values of $\rho(\mathbf{r})$ function (0.237−0.491 eÅ^{-3}) point out that they are much stronger than the K−O bonds. Indeed, their energy is 13.0−15.0 kcal/mol for the anion−anion H-bonds and it even reaches 30 kcal/mol for the cation−anion ones (Table 2). The strength of the latter, clearly, defines the high degree of the charge transfer from hydrogensulfates to the oxonium species. The total energy of the cation−anion H-bonds formed by the S(1)O$_4$H$^-$ moiety reaches 29.1 kcal/mol, whereas for the other anion it is 26.9 kcal/mol. On the one hand, these values seem to disagree with the common trend for the ionic H-bonds[2,34] because the stronger the H-bonds with oxonium cation in **1**, the more negatively charged (by ca. 0.2 e) is the hydrogensulfate moiety. However, if we consider only SO$_3$ fragments directly involved in the H-bonding, the difference in their charges (−0.15 and −0.05 e for S(1)O$_3$ and S(2)O$_3$ groups) reduces down to 0.1 e with the total energy remaining the same. Moreover, the sums of S−O bond lengths, which can also provide the quantitative information on the charge transfer in the crystalline salts,[35] are very close to each other and are equal to 4.363 and 4.366 Å for the S(1)O$_3$ and S(2)O$_3$ species. The total energy of the cation−anion H-bonds per H$_3$O$^+$ moiety is 56 kcal/mol. Its charge increases by 0.75 e upon their formation. These values are rather reasonable, for instance, compared with those for the close-ion pair of guanidinium chloride,[34] in the crystals of 1,5-naphthalenedisulfonic acid tetrahydrate[35] and hydroxyl ammonium chloride.[36] The charge transfer and the total energy of the cation−anion H-bonds for these systems are 0.22, 0.55, 0.72 e and 9.8, 51.0, 45.2 kcal/mol, respectively.

The supramolecular organization of ions in the crystal of **1** includes very weak O···O interactions (O···O 3.1983(15)−3.5260(15) Å) between both the symmetrically related and independent anions. It is to be mentioned that the similar self-assembly of nitrate moieties in the crystalline uronium nitrate[37] is characterized by the O···O interatomic separation of 3.0814(4) Å and the energy of 1.4 kcal/mol. The topological characteristics of these bonds in **1** ($\nabla^2\rho(\mathbf{r}) = 0.06 - 0.46$ eÅ^{-5}, $h_e(\mathbf{r}) = 0.00019 - 0.00131$ au) allow classifying them as closed-shell interactions. However, the degree of the electron density accumulation in their BCPs is even smaller than that for the K−O bonds. Thus, given the presence of the strong H-bonds in **1**, the influence of such O···O interactions on the hydrogensulfate ions can be neglected because their energy is less than 1.7 kcal/mol and amounts to 5.8 kcal/mol in total. The same holds for the additional cation−anion interaction (Figure 6) linking the O$_{ox}$(9) atom with the oxygen of the S(1)O$_4$H$^-$ anion. In this case, the E_{int} value is 1.4 kcal/mol with the $\nabla^2\rho(\mathbf{r})$ and $h_e(\mathbf{r})$ equal to 0.76 eÅ^{-5} and 0.00177 au. Hence, the O$_{ox}$(9) atom in **1** forms only one nondirectional O$_{ox}$···O bond rather than interacts with the proton-donor groups. The inspection of the DED distribution function in the interatomic area (Figure 6) shows that the O(4) atom donates the electron density to the oxygen site of the oxonium moiety and not the reverse.

To understand the reasons for such a behavior of the oxonium cation, we turn to the analysis of the Laplacian of the electron density distribution $\nabla^2\rho(\mathbf{r})$ in the vicinity of the O$_{ox}$(9) atom. The search for the CP (3, −3) of the $-\nabla^2\rho(\mathbf{r})$ function revealed no maximum attributed to the LP of the oxygen atom in **1**. The failure of its localization can be due to the compactness of this lone pair. The absence of the expected CPs (3, −3) in the $-\nabla^2\rho(\mathbf{r})$ function was also observed in the theoretical study of phosphinoxides,[38] in

TABLE 2: Topological Parameters of the Experimental $\rho(\mathbf{r})$ Function in BCPs of the Interionic Interactions in 1

interaction[a]	d^b, Å	$\rho(\mathbf{r})$, eÅ^{-3}	$\nabla^2\rho(\mathbf{r})$, eÅ^{-5}	$-v(\mathbf{r})$, au	$h_e(\mathbf{r})$, au	E_{int}, kcal/mol
K(1)−O(1)	2.7620(15)	0.070	1.81	0.00911	0.00484	2.9
K(1)−O(2)	2.9657(12)	0.105	0.71	0.00803	0.00035	2.5
K(1)−O(2")	2.6906(11)	0.121	1.94	0.01382	0.00317	4.3
K(1)−O(3**A**)	2.7467(13)	0.100	1.65	0.01083	0.00315	3.4
K(1)−O(5′)	2.6944(13)	0.177	1.61	0.01882	0.00104	5.9
K(1)−O(6)	2.7953(15)	0.069	1.49	0.00792	0.00376	2.5
K(1)−O(8**B**)	2.7665(14)	0.080	1.55	0.00889	0.00361	2.8
O(1)···H(4**C**)	2.5938(16)	0.254	4.96	0.04149	0.00496	13.0
O(1)···O(5**D**)	3.3971(15)	0.052	0.30	0.00275	0.00019	0.9
O(2)···O(2**E**)	3.3512(14)	0.095	0.12	0.00512	0.00193	1.6
O(3)···H(9A**F**)	2.5310(16)	0.491	5.71	0.09263	−0.01669	29.1
O(3)···O(8**G**)	3.1983(15)	0.027	0.39	0.00192	0.00104	0.6
O(4)···O(6**H**)	3.3979(16)	0.046	0.40	0.00278	0.00066	0.9
O(4)···O(9**B**)	3.0574(14)	0.052	0.76	0.00439	0.00177	1.4
O(4)···O(8**H**)	3.1992(15)	0.038	0.46	0.00261	0.00106	0.8
O(5)···O(5**D**)	3.5260(15)	0.073	0.06	0.00326	0.00131	1.0
O(7)···H(9C)	2.6740(16)	0.273	4.78	0.04390	0.00285	13.8
O(7)···H(6**I**)	2.6480(16)	0.341	2.34	0.04767	−0.00117	15.0
O(8)···H(9B**J**)	2.5994(16)	0.237	5.82	0.04169	0.09344	13.1

[a] The atoms with asterisks are obtained from the basic ones by the symmetry operations $-x+1, 1.5+y, 1.5-z$ and $-x+1, 1.5+y, 2.5-z$. The atoms labeled with **A**, **B**, and **C** are obtained from the basic ones by the symmetry operations $-x+1, -1-y, 1-z$; $-1+x, y, z$ and $x, 0.5-y, -0.5+z$. The atoms labeled with **D**, **E**, and **F** are obtained from the basic ones by the symmetry operations $-x+1, -y+1, -z+1$; $-x+1, -y+1, -z+1$ and $x, 0.5-y, -1.5+z$. The atoms labeled with **G**, **H**, and **I** are obtained from the basic ones by the symmetry operations $-x+2, 0.5+y, 1.5-z$; $-x+1, 0.5+y, 1.5-z$ and $-x+2, 1.5+y, 2.5-z$. The H(9B**J**) atom is obtained from the basic one via the symmetry operation $-x+2, -y, -z+1$. [b] When the O···H contacts are concerned, d stands for the O···O distance.

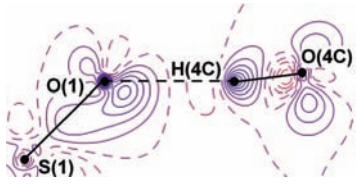

Figure 4. DED distribution in the plane of the O(1), H(4C) and O(4C) atoms in the crystal of **1**. The contours are drawn with 0.1 eÅ^{-3} step, the nonpositive contours are dashed.

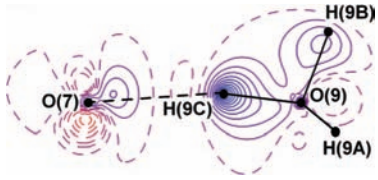

Figure 5. The DED distribution in the plane of the O(7), H(9C), and O(9) atoms in the crystal of **1**. The contours are drawn with 0.1 eÅ^{-3} step, the nonpositive contours are dashed.

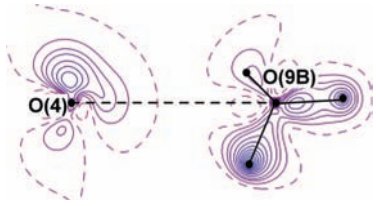

Figure 6. DED distribution in the area of the O_{ox}···O interaction in the crystal of **1**. The contours are drawn with 0.1 eÅ^{-3} step, the nonpositive contours are dashed.

which these critical points would have been close to the atomic nuclei. The examination of the ELF,[39] which is theoretically more sound for the localization of electron pair domains,[39,40] shows the electron density accumulation very close to the oxygen nucleus (Figure 7). Although the reliability of the experimental, that is approximate, ELF was questioned,[41] it was shown that the LP domains can be unambiguously localized via its analysis.[42−45] Indeed, careful

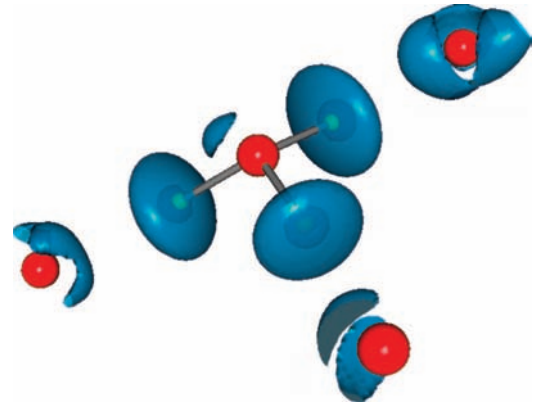

Figure 7. 3D distribution of ELF around the oxonium ion showing the LP of the oxygen atom. Isosurface of ELF equal to 0.8 is shown in blue.

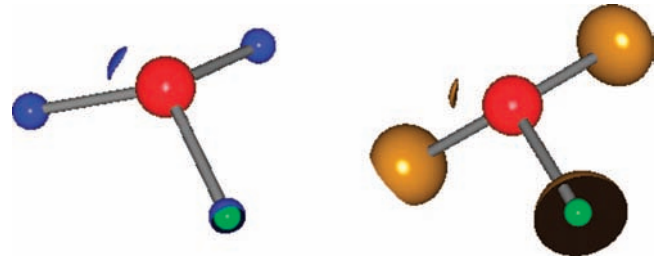

Figure 8. 3D distribution of $-\nabla^2\rho(\mathbf{r})$ (**A**) and LOL (**B**) functions around the oxonium ion showing the LP of the oxygen atom. Isosurface of $-\nabla^2\rho(\mathbf{r})$ function equal to 108 eÅ^{-5} is shown in blue. Isosurface of LOL equal to 0.6 is shown in yellow.

examination of the 3D distribution of the $-\nabla^2\rho(\mathbf{r})$ (part A of Figure 8) as well as the LOL function[44,46,47] (part B of Figure 8) revealed exactly the same trends as for the ELF. In all cases, the LP of the O(9) atom was found to be very compact. On the contrary, LPs around the oxygen atoms of the hydrogensulfate moieties (Figure 9) are relatively diffuse. The presence of three LPs in the valence shells of the proton-

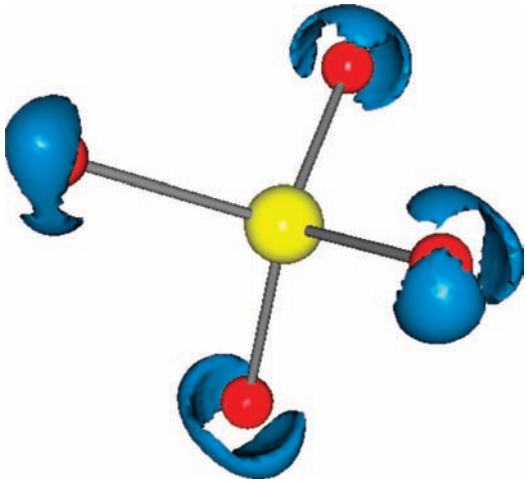

Figure 9. 3D distribution of ELF within the anionic $S(1)O_4H$ moiety. The hydrogen atom of the O(4) oxygen (left) is not shown. Isosurface of ELF equal to 0.8 is shown in blue.

free oxygen atoms of the anions is indicative of the single-bonded character of the S−O bonds. This is in a good agreement with low values of the ellipticity ($\varepsilon = 0.031-0.088$) in the corresponding BCPs, which are similar to those for the Cl−O and P−O bonds in sodium chlorate[48] and diphenylphosphonic acid,[42] respectively. In addition to the compactness, the lone pair domain of the O_{ox} atom in **1** is also tilted toward the H(9A) atom, which is moved away from the O(4) atom, that allow the O(9)···O(4) interaction to form via the charge transfer from the second oxygen to the σ^*-orbital of the O(9)−H(9A) bond. These electronic and structural features of the H_3O^+ moiety are, apparently, responsible for the tendency of the H_3O^+ oxygen atom to avoid the H-bond formation.

Conclusion

High-resolution X-ray diffraction study of the crystalline potassium oxonium bis(hydrogensulfate) has revealed a complicated H-bonded network comprising cation−anion and anion−anion interactions of different types. They result in a significant charge transfer to the oxonium cation, which makes this moiety electronically close to water molecule. At the same time, no H-bond involving the oxygen atom of the oxonium as a proton acceptor was found. This feature is well-known and persists in almost all oxonium salts. It was shown that it is due to the compact character of the only lone pair of the oxonium. This electron pair domain cannot be found via topological analysis of $\nabla^2\rho(\mathbf{r})$ function but was unambiguously visualized basing on 3D ELF mapping. Moreover, its compactness allows for the formation of a weak O···O interaction with anion. Therefore, one should not expect that even the modification of counterions could effectively make the H_3O^+ moiety a proton acceptor in designing supramolecular networks of proton conducting materials.

Acknowledgment. This study was financially supported by the Russian Foundation for Basic Research (Project 09-03-00603-0), the Foundation of the President of the Russian Federation (Federal Program for the Support of Leading Scientific Schools, Grant NSh 1060.2003.30, and Young Doctors, Grant MK-1054.2005.3), and the Russian Science Support Foundation. Authors also thank Dr. I. V. Glukhov for fruitful discussion.

Supporting Information Available: Tables of monopole, dipole, and quadrupole populations, table of differences of mean-squares displacement amplitudes, and a residual electron density map. This material is available free of charge via the Internet at http://pubs.acs.org.

References and Notes

(1) Muller-Dethlefs, K.; Hobza, P.; Reschel, T. *Chem. Rev.* **2000**, *100*, 143.
(2) Meot-Ner, M. *Chem. Rev.* **2005**, *105*, 213.
(3) Braga, D.; Maini, L.; Polito, M.; Grepioni, F. Hydrogen bonding interactions between ions: A powerful tool in molecular crystal engineering. I. *Supramolecular Assembly Via Hydrogen Bonds II* **2004**, *111*, 1.
(4) Desiraju, G. R. *Crystal Engineering: The Design of Organic Solids*; Elsevier: Amsterdam, 1989.
(5) Desiraju, G. R. J. Chem. Soc., Dalton Trans. **2000**, p 3745.
(6) Desiraju, G. R.; Steiner, T. The Weak Hydrogen Bond in Structural Chemistry and Biology; Oxford University Press: New York, 1999.
(7) Kreuer, K. D. *Proton Conductivity: Materials and Applications* **1996**, *8*, 610.
(8) Cambridge Crystallographic Database (version 5.29). 2008.
(9) Fabbiani, F. P. A.; Allan, D. R.; Dawson, A.; Francis, D. J.; Marshall, W. G.; Pulham, C. R. *Inorg. Chim. Acta* **2008**, *361*, 487.
(10) Boese, R.; Niederprum, N.; Blaser, D.; Maulitz, A.; Antipin, M. Y.; Mallinson, P. R. *J. Phys. Chem. B* **1997**, *101*, 5794.
(11) Koritsanszky, T. S.; Coppens, P. *Chem. Rev.* **2001**, *101*, 1583.
(12) Gatti, C. *Z. Kristallogr.* **2005**, *220*, 399.
(13) Tsirelson, V. G.; Ozerov, R. P. *Electron density and Bonding in Crystals: Principles, Theory and X-Ray Diffraction experiments in Solid State Physics And Chemistry*; IOP Publishing Ltd.: Bristol and Philadelphia, 1996.
(14) Kemnitz, E.; Werner, C.; Trojanov, S.; Worzala, H. *Z. Anorg. Allg. Chem.* **1994**, *620*, 1921.
(15) Bader, R. F. W. *Atoms In molecules. A Quantum Theory*; Clarendron Press: Oxford, 1990.
(16) Espinosa, E.; Molins, E.; Lecomte, C. *Chem. Phys. Lett.* **1998**, *285*, 170.
(17) Espinosa, E.; Alkorta, I.; Rozas, I.; Elguero, J.; Molins, E. *Chem. Phys. Lett.* **2001**, *336*, 457.
(18) Sheldrick, G. M. *SHELXTL v. 5.10, Structure Determination Software Suit*; Bruker AXS: Madison, Wisconsin, USA.
(19) Hansen, N. K.; Coppens, P. *Acta Crystallogr. A* **1978**, *34*, 909.
(20) Koritsansky, T. S.; Howar, S. T.; Richter, T.; Mallinson, P. R.; Su, Z.; Hansen, N. K. XD, a computer program package for multipole refinement and analysis of charge densities from X-ray diffraction data, 1995.
(21) Su, Z. W.; Coppens, P. *Acta Crystallogr., Sect. A* **1995**, *51*, 27.
(22) Kirzhnits, D. A. *Sov. Phys. JETP* **1957**, *5*, 54.
(23) Stash, A.; Tsirelson, V. *J. Appl. Crystallogr.* **2002**, *35*, 371.
(24) Lyssenko, K. A.; Nelyubina, Y. V.; Kostyanovsky, R. G.; Antipin, M. Y. *ChemPhysChem* **2006**, *7*, 2453.
(25) Puntus, L. N.; Lyssenko, K. A.; Antipin, M. Y.; Bunzli, J.-C. G. *Inorg. Chem.* **2008**, *47*, 11095.
(26) Nelyubina, Y. V.; Lyssenko, K. A.; Antipin, M. Y. *Crystallogr. Reports* **2008**, *53*, 192.
(27) Nelyubina, Y. V.; Antipin, M. Y.; Lyssenko, K. A. *CrystEngComm.* **2007**, *8*, 632.
(28) Pidko, E. A.; Xu, J.; Mojet, B. L.; Lefferts, L.; Subbotina, I. R.; Kazansky, V. B.; van Santen, R. A. *J. Phys. Chem. B* **2006**, *110*, 22618.
(29) Pidko, E. A.; van Santen, R. A. *ChemPhysChem* **2006**, *7*, 1657.
(30) Lyssenko, K. A.; Antipin, M. Y. *Russ. Chem. Bull.* **2006**, *55*, 1–15.
(31) Sobczyk, L.; Grabowski, S. J.; Krygowski, T. M. *Chem. Rev.* **2005**, *105*, 3513.
(32) Borissova, A. O.; Korlyukov, A. A.; Antipin, M. Yu.; Lyssenko, K. A. *J. Phys. Chem. A* **2008**, *112*, 11519–11522.
(33) Lyssenko, K. A.; Antipin, M. Y. *Russ. Chem. Bull.* **2006**, *55*, 1.
(34) Rozas, I.; Kruger, P. E. *J. Chem. Theory Comput.* **2005**, *1*, 1055.
(35) Lyssenko, K. A.; Barzilovich, P. Y.; Aldoshin, S. M.; Antipin, M. Y.; Dobrovolsky, Y. A. *Mendeleev Commun.* **2008**, *18*, 312.
(36) Nelyubina, Y. V.; Antipin, M. Y.; Lyssenko, K. A. *J. Phys. Chem. A* **2007**, *111*, 1091.
(37) Nelyubina, Y. V.; Lyssenko, K. A.; Golovanov, D. G.; Antipin, M. Y. *CrystEngComm* **2007**, *9*, 991.
(38) Dobado, J. A.; Martinez-Garcia, H.; Molina, J. M.; Sundberg, M. R. *J. Am. Chem. Soc.* **1998**, *120*, 8461.
(39) Tsirelson, V.; Stash, A. *Chem. Phys. Lett.* **2002**, *351*, 142.
(40) Savin, A.; Nesper, R.; Wengert, S.; Fassler, T. F. *Angew. Chem., Int. Ed. Engl.* **1997**, *36*, 1809.
(41) Jayatilaka, D.; Grimwood, D. *Acta Crystallogr., Sect. A* **2004**, *60*, 111.

(42) Lyssenko, K. A.; Grintselev-Knyazev, G. V.; Antipin, M. Y. Mendeleev Commun. **2002**, 128.
(43) Lyssenko, K. A.; Aldoshin, S. M.; Antipin, M. Y. *Mendeleev Commun.* **2004**, *98*, 101.
(44) Lyssenko, K. A.; Antipin, M. Y.; Gurskii, M. E.; Bubnov, Y. N.; Karionova, A. L.; Boese, R. *Chem. Phys. Lett.* **2004**, *384*, 40–44.
(45) Lyssenko, K. A.; Odinets, I. L.; Kazakov, P. V.; Pasechnik, M. P.; Antipin, M. Yu *Russ. Chem. Bull.* **2005**, *54*, 560–565.
(46) Schmider, H. L.; Becke, A. D. *J. Mol. Structure (Theochem)* **2000**, *527*, 51–61.
(47) Tsirelson, V.; Stash, A. *Acta Crystallogr., Sect. B* **2002**, *58*, 780–785.
(48) Nelyubina, Y. V.; Lyssenko, K. A.; Kostyanovsky, R. G.; Bakulin, D. A.; Antipin, M. Y. *Mendeleev Commun.* **2008**, *18*, 29.

JP900215H